# Modelling of Rock-Shotcrete Interfaces Using a Novel Bolted Cohesive Element

Ali Karrech(✉) and Xiangjian Dong

Department of Civil, Environmental and Mining Engineering, School of Engineering, The University of Western Australia, 35 Stirling Hwy, Crawley, WA 6009, Australia
ali.karrech@uwa.edu.au

**Abstract.** Rock-shotcrete interfaces are commonly encountered in mining and civil engineering infrastructures, which can trigger localised failure due to stress concentration. These interfaces are usually reinforced with support systems such as rock bolts and the behaviour of rock-shotcrete-bolt systems is often difficult to predict mechanically. In this study, we introduce a new technique to model rock-shotcrete interfaces embedding rock bolts using the finite element method. The proposed approach is implemented in the general purpose simulation package Abaqus via its user-defined element (UEL) subroutine. The proposed model takes into account the uneven interface roughness and the complex interaction between its components. The cohesive stiffness of the model degrades proportionally to the damage that occurs due to this interaction. The stiffness of the bolt connection and its location are also considered in the proposed mathematical formulation. The present bolted cohesive element has been validated experimentally; good agreement has been obtained between the measurement and numerical simulation under the conditions of direct shear test and bolt pull-out tests. Mesh independence has also been verified by examining the effect of mesh size on the overall force-displacement response of typical structures. With the model at hand, the effects of key installation parameters such as number of bolts, their inclinations and material properties have been investigated.

**Keywords:** Interface · Rock-shotcrete · Finite element method · User-defined element · Cohesive element

## 1 Introduction

Rock-shotcrete interfaces are common in mining and civil engineering infrastructures including underground tunnels and excavations. These interfaces are important to investigate since they represent irregularities that usually cause stress concentration. Factors such as rock roughness, shotcreting irregularities, properties of reinforcing elements (e.g. rock bolts and/or fibres), and the conditions of their installation influence the behaviour of these interfaces. These irregularities can be attributed to the heterogenous nature of rocks and also to


P. Rossi and J.-L. Tailhan (Eds.): SSCS 2022, RILEM Bookseries 38, pp. 170–177, 2023.
https://doi.org/10.1007/978-3-031-07746-3_17

the excavation process that is often based on drilling and blasting or mechanical digging, which makes it difficult to obtain smooth surfaces free of local defects. Shotcrete is usually sprayed on these surfaces to prevent detachment of loose rocks, especially in the presence of workers and/or heavy equipment. Naturally, shotcrete spraying results in non-uniform layers that slightly smoothen the original rock surface and strengthen it. The interface between the rock mass and the shotcrete layer relies essentially on the bounding that occur due to cement hydration reactions. Additional strength is gained by reinforcing the structure with rock bolts.

To the author's knowledge there are no cohesive element approaches in the literature to predict the behaviour of rock- shotcrete interfaces, especially when support systems such as rock bolts are used. Existing approaches to predict the behaviour of rock-shotcrete interfaces are essentially analytical as shown by the authors in previous contributions [1,2] and they ignore the effect of reinforcing systems. The present formulation builds on a similar element that the authors suggested for fiber-reinforced concrete [2]. However, the different scales between fibers and bolts as well as the absence of interface in plain concrete make this approach fairly different. It is worthwhile noting that the proposed formulation does not apply only to mining and civil engineering infrastructures embedding such interfaces but also to other applications where detachment between different materials can occur in a localised manner.

In this study, we introduce a new technique to model rock-shotcrete interfaces embedding rock bolts using the finite element method. We developed a so called "bolted cohesive element" through the user-defined element (UEL) subroutine of Abaqus to describe this complex interface. The proposed model takes into account the uneven interface roughness and the complex interaction between its components.

## 2 Bolted Cohesive Element Model

Cohesive modelling was introduced by Dugdale and Barenblatt [3,4] in 1960 s s and it has been applied to various engineering problems [5–7]. It describes joints or interfaces that differ from the bulk materials that surround them in terms of mechanical behaviour. The governing equations are derived from the principle of virtual work which reads

$$\int_{\Omega} \boldsymbol{\sigma}^T \delta \boldsymbol{\varepsilon} d\Omega + \int_{\Gamma_c} \boldsymbol{T_c}^T \delta \boldsymbol{\Delta} dS = \int_{\Gamma_e} \boldsymbol{T_e}^T \delta \boldsymbol{u} dS \qquad (1)$$

where $\boldsymbol{\sigma}$, $\delta\boldsymbol{\varepsilon}$, $\delta\boldsymbol{\Delta}$ and $\delta\boldsymbol{u}$ represent Cauchy stress, virtual strain, virtual separation and virtual displacement field, respectively. The principle is applied within a 3D domain $\Omega$ embedding a cohesive region $\Gamma_c$ as shown in Fig. 1. External forces $\boldsymbol{T_e}$ and/or essential boundary conditions $\boldsymbol{u}$ are applied through the surface $\Gamma_e$. The contribution of body forces is neglected in this formulation.

At the crack interface ($\Gamma_c$), the cohesive traction $\boldsymbol{T_c}$ is related to the relative separation between the interface boundaries $\boldsymbol{\Delta}$ by:

$$\boldsymbol{T_c} = \boldsymbol{D_c} \ \boldsymbol{\Delta} \qquad (2)$$

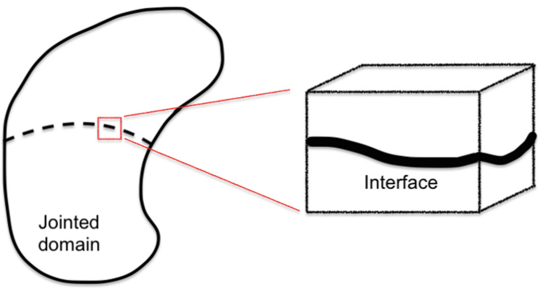


**Fig. 1.** Schematic representation of a 3D cohesive element.

where the constitutive matrix $\boldsymbol{D_c}$ is determined experimentally. Embedding a bolt into the interface at a location $(x_b, y_b, z_b)$ and applying a pretension force $\boldsymbol{P_0}$ (see in Fig. 2), results in the following expression

$$\int_{\Omega} \boldsymbol{\sigma}^T \delta \boldsymbol{\varepsilon} dV + \int_{\Gamma_c} \boldsymbol{T_c}^T \delta \boldsymbol{\Delta} dS + \int_{\Gamma_c} \boldsymbol{T_b}^T \delta \boldsymbol{\Delta} \delta(x - x_b, y - y_b, z - z_b) dS = \int_{\Gamma_e} \boldsymbol{T_e}^T \delta \boldsymbol{u} dS + \int_{\Gamma_c} \boldsymbol{P_0}^T \delta \boldsymbol{u} dS \tag{3}$$

where $\boldsymbol{T_b}$ is an internal point load that equilibrates the bolt pretension and $\delta(x - x_b, y - y_b, z - z_b)$ is the Dirac delta function.

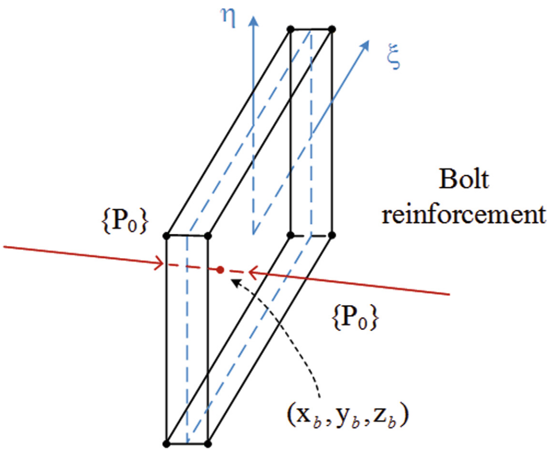


**Fig. 2.** Cohesive element with pre-stressed bolt reinforcement.

Based on Eq. (3) it can be shown that each cohesive element is governed by $\boldsymbol{Kd} = \boldsymbol{F}$, where $\boldsymbol{K}$ is the stiffness matrix, $\boldsymbol{d}$ is the vector of degrees of freedom, and $\boldsymbol{F}$ is the vector of nodal forces. It can be shown that the stiffness matrix is

$$\boldsymbol{K} = \int_{-1}^{1}\int_{-1}^{1} \tilde{\boldsymbol{B}}^T \boldsymbol{D}_{local} \tilde{\boldsymbol{B}} |\boldsymbol{J}| d\xi d\eta + \int_{-1}^{1}\int_{-1}^{1} \delta(\boldsymbol{\xi} - \boldsymbol{\xi}_b) \tilde{\boldsymbol{B}}^T \boldsymbol{D}_s \tilde{\boldsymbol{B}} d\xi d\eta \tag{4}$$

where $\tilde{\boldsymbol{B}} = \boldsymbol{RB}$ and $\boldsymbol{R}$ is a rotation matrix. The first term of Eq. (4) represents the cohesive stiffness and the second denotes the bolt stiffness. Similarly, the vector of nodal forces reads

$$\begin{aligned} \boldsymbol{F} = &\int_{-1}^{1}\int_{-1}^{1} \boldsymbol{B}^T \boldsymbol{R}^T \boldsymbol{T_c} |\boldsymbol{J}| d\xi d\eta + \int_{-1}^{1}\int_{-1}^{1} \boldsymbol{B}^T \boldsymbol{R}^T \boldsymbol{T_b} \delta(\xi - \xi_b, \eta - \eta_b) d\xi d\eta \\ &+ \int_{-1}^{1}\int_{-1}^{1} \delta(\boldsymbol{\xi} - \boldsymbol{\xi}_b) \tilde{\boldsymbol{B}}^T \boldsymbol{P}_0 d\xi d\eta \end{aligned} \tag{5}$$

The vector of nodal forces includes the effects of cohesive traction, bolt force, and initial pretension applied on the bolt which are the three terms of Eq. (5), respectively. The last term can be expressed by

$$\boldsymbol{F^e}_p = \boldsymbol{B}_{(\xi_b, \eta_b)} \boldsymbol{R P}_0 \tag{6}$$

The rock-shotcrete interface has a complex structure with uneven interface behaviour as illustrated in Fig. 2-a. The response of this interface is governed by a multi-dimensional stiffness having normal ($K_n$) and shear ($K_t$) components. Given the uneven interface, $K_t$ is further decomposed into cohesion and friction components. The interface behaviour can be measured by using normal loading tests [8], static Brazilian disc split tests [9] and direct shear tests [10], respectively. A bilinear traction-separation law is adopted for the normal traction component in this simulation. In addition, a mixed 'cohesive' and 'Coulomb-friction' model is used to approximate the non-linear behaviour of rock-shotcrete interfaces. This results in a three-stages behaviour that includes elastic, bond failure and friction sliding regions, as suggested by [10]. As shown in Fig. 2-b, the shear traction increases linearly with displacement until it reaches the onset of failure ($T'_{max}$) at a displacement $\delta_0$. Beyond this threshold, the shear traction reduces non linearly until $T'_{max}$ is reached at a displacement $\delta_c$. A residual shear stress is then maintained as displacement increases.

The degradation of the cohesive stiffness is described with the damage variable $D$, which varies from zero to one and can be expressed as a function of displacement as follows

$$D = \begin{cases} 0, & for \quad \delta < \delta_0 \\ f(\delta), & for \quad \delta_0 \leqslant \delta < \delta_c \\ 1, & for \quad \delta \geqslant \delta_c \end{cases} \tag{7}$$

where the function $f(\delta)$ is fitted experimentally to reflect the effects of material strength and joint roughness. A quintic polynomial function is used in the current

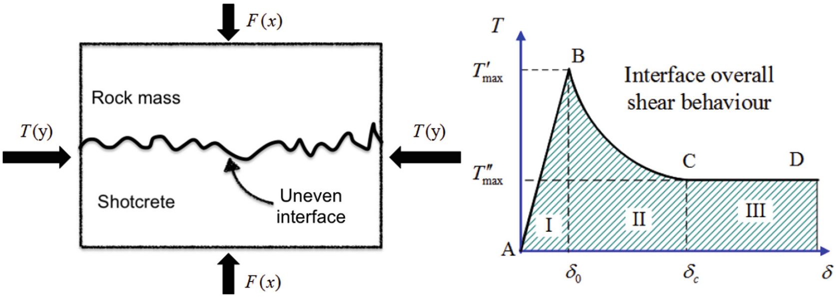


**Fig. 3.** Illustrations of (a) uneven rock-liner interface and (b) interface shear constitutive model.

case. In addition, we considered that the shear stiffnesses in the two tangential directions are equal which leads to the following constitutive relation for the shear component:

$$T_c = \begin{cases} k_s^c \delta, & for \quad \delta < \delta_0 \\ k_s^c(1 - f(\delta))\delta + k_{fs}^c \delta, & for \quad \delta_0 \leqslant \delta < \delta_c \\ \mu_n T_n, & for \quad \delta \geqslant \delta_c \end{cases} \tag{8}$$

where $k_s^c = T'_{max}/\delta_0$ and $k_{fs}^c = T''_{max}/(\delta_c - \delta_0))$.

## 3 Results and Discussion

Before the model can be used for field applications, simple cases of loading are considered for validation. The first case simulates a simple shear test and the results are compared to published experimental data [10]. Cubic specimens of size 150 $mm$ with artificial rock-concrete interfaces are considered. The specimens are subjected to shear displacement at a rate of 0.005 $mm/s$ under a normal compression stress of 4 $MPa$. The bulk material is assumed to have an elastic modulus of 21 $GPa$ and a Poisson ratio of 0.3. The friction coefficient at the interface is set to $\mu_n = 0.8$ and the joint roughness coefficient (JRC) of the interface is less than 2. The measured normal compression and residual stresses are 4 $MPa$ and 3.2 $MPa$, respectively. Figure 3-a shows the reaction force over the area of shear interface versus applied shear displacement. It can be seen that a good agreement is obtained between the proposed model and the experimental test. As a second validation case, a single bolt pull-out test is simulated and the results are compared to published experimental data [11]. The pull-out tests were conducted using an MTS Criterion 60 testing machine; a bolt of 20 $mm$ in diameter is inserted into a steel tube and bonded with resin. Resin-based bolting is widely used by the mining industry to ensure fast curing (the mixture solidifies in minutes unlike cement bolting). Again, excellent agreement was obtained between the numerical and experimental data, as shown in Fig. 3-b.

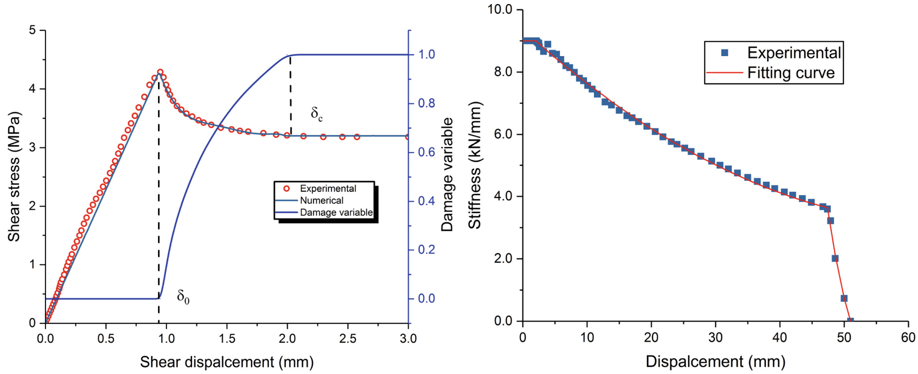


**Fig. 4.** Model validation for (a) direct shear test and (b) normal stiffness of the resin bonded bolt system.

After validation using the direct shear and single bolt pull-out tests, the model was used to conduct a parametric study. The first parameter of interest is the number of bolts within a given interface, as the common practice in engineering infrastructures is to apply more than one bolt to enhance the overall behaviour of support systems. Figure 5-a shows the response of the structure with respect to displacement for various numbers of bolts. It can be seen that the total force increases with the number of bolts, which suggests that the denser the bolts, the higher the shear resistance of the system. However, Fig. 5-b indicates that the average force does not change much with the number of bolts. This means that the overall force increases linearly with the bolt numbers.

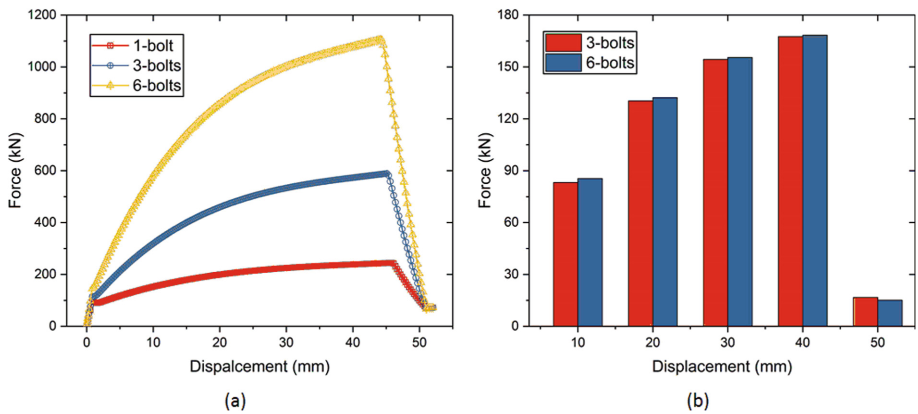


**Fig. 5.** The effect of bolt number (a) overall force variation against displacement (b) average force increase under 3 and 6 bolts situations.

Another key parameter that influences the performance of bolt-based support systems is the bolt installation angle. This is the angle between the bolt orientation and the normal direction of the interface. Figure 6 shows the shear force versus displacement at various bolt installation angles. It can be seen that the force increases with the installation angle and reduces abruptly when the bolt fails. The results indicate that the higher the installation angle the stiffer the bolted system. Similar results were obtained experimentally and reported in previous studies by Dight [12] and Li et al. [13].

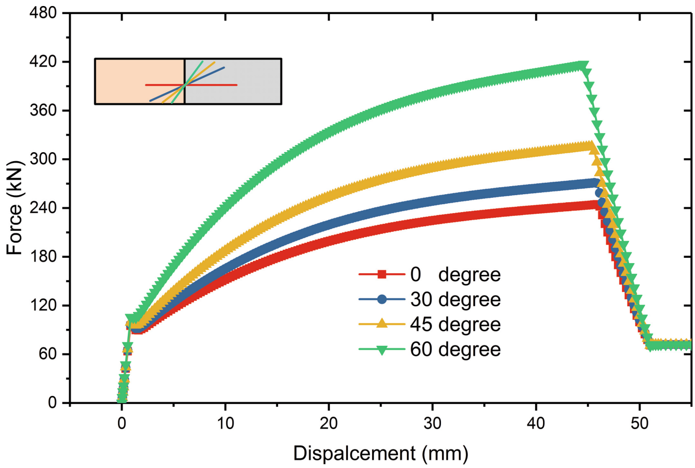


**Fig. 6.** The shear force variation under the effect of bolt installation angle.

## 4 Conclusions

A novel bolted cohesive element has been introduced to model support systems of rock bolts reinforcing shotcrete applied to underground excavations. The proposed element has been implemented using the Fortran user element subroutine UEL of ABAQUS. The model was validated using direct shear and bolt pull-out tests and it showed excellent agreement between the experimental data and the numerical results. Based on this model, a parametric study has shown that the overall behaviour of the system is strongly influences by the geometry of bolt installation. The model has indicated that the shear resistance of the system increases linearly with the number of reinforcing bolts. In addition, the model has als shown that increasing the installation angle increases the effective stiffness of the system and its overall strength.

## References


1. Dong, X., Karrech, A., Elchalakani, M., Qi, C., Manka, M.: 3D bolted cohesive element for the modelling of bolt-reinforced rough rock-shotcrete interfaces. Comput. Geotech. **125**, 103659 (2020)
2. Manka, M., Karrech, A., Dight, P., Ciancio, D.: Dual cohesive elements for 3D modelling of synthetic fibre-reinforced concrete. Eng. Struct. **174**, 851–860 (2018)
3. Dugdale, D.S.: Yielding of steel sheets containing slits. J. Mech. Phys. Solids **8**(2), 100–104 (1960)
4. Barenblatt, G.I.: The mathematical theory of equilibrium cracks in brittle fracture. In: Advances in Applied Mechanics, Vol. 7, pp. 55–129. Elsevier (1962)
5. Park, K., Paulino, G.H.: Cohesive zone models: a critical review of traction-separation relationships across fracture surfaces. Appl. Mech. Rev. **64**(6), 060802 (2011)
6. Park, K., Paulino, G.H.: Computational implementation of the ppr potential-based cohesive model in abaqus: educational perspective. Eng. Fract. Mech. **93**, 239–262 (2012)
7. Spring, D.W., Paulino, G.H.: A growing library of three-dimensional cohesive elements for use in abaqus. Eng. Fract. Mech. **126**, 190–216 (2014)
8. Bae, G., Chang, S., Lee, S., Park, H.: Evaluation of interfacial properties between rock mass and shotcrete. Int. J. Rock Mech. Min. Sci. **41**, 106–112 (2004)
9. Luo, L., Li, X., Tao, M., Dong, L.: Mechanical behavior of rock-shotcrete interface under static and dynamic tensile loads. Tunn. Undergr. Space Technol. **65**, 215–224 (2017)
10. Tian, H., Chen, W., Yang, D., Yang, J.: Experimental and numerical analysis of the shear behaviour of cemented concrete-rock joints. Rock Mech. Rock Eng. **48**(1), 213–222 (2015)
11. Feng, X., Zhang, N., Yang, S., He, F.: Mechanical response of fully bonded bolts under cyclic load. Int. J. Rock Mech. Min. Sci. **109**, 138–154 (2018)
12. P. Dight, A case study of the behaviour of rock slope reinforced with fully grouted rock bolts. In: Proceedings International Symposium on Rock Bolting, Abisko, Sweden, pp. 523–538 (1983)
13. Li, L., Hagan, P., Saydam, S., Hebblewhite, B., Li, Y.: Parametric study of rockbolt shear behaviour by double shear test. Rock Mech. Rock Eng. **49**(12), 4787–4797 (2016)